

Article

Barium Lanthanum Oxide Nanosheets in Photocatalytic and Forensic Applications: One-Pot Synthesis and Characterization

Sanjay S. Majani ¹, Meghana ¹, Sowmyashree S H ¹, Sowjanyaashree J ¹, Sahaja Umesh ¹, Chandan Shivamallu ² , Muzaffar Iqbal ³ , Raghavendra G. Amachawadi ⁴ , Venkatachalaiah K N ^{5,*} and Shiva Prasad Kollur ^{1,*} 

¹ School of Physical Sciences, Amrita Vishwa Vidyapeetham, Mysuru Campus, Mysuru 570 022, Karnataka, India; sanjaymajani05@gmail.com (S.S.M.)

² Department of Biotechnology and Bioinformatics, JSS Academy of Higher Education and Research, Mysuru 570 015, Karnataka, India; chandans@jssuni.edu.in

³ Department of Pharmaceutical Chemistry, College of Pharmacy, King Saud University, Riyadh 11451, Saudi Arabia

⁴ Department of Clinical Sciences, College of Veterinary Medicine, Kansas State University, Manhattan, KS 66506-5606, USA; agraghav@vet.k-state.edu

⁵ Department of Physics, Amrita School of Engineering, Amrita Vishwa Vidyapeetham, Bengaluru Campus, Bengaluru 560 035, Karnataka, India

* Correspondence: kn_venkatachalaiah@blr.amrita.edu (V.K.N.); shivachemist@gmail.com (S.P.K.)

Abstract: The present work elucidates the fabrication of Barium Lanthanum Oxide nanosheets (BaLa₂O₄ NSs) via a simple one-pot precipitation method. The acquired results show an orthorhombic crystal system with an average crystallite size of 27 nm. The morphological studies revealed irregular-shaped sheets stacked together in a layered structure, with the confirmation of the precursor elements. The diffused reflectance studies revealed a strong absorption between 200 nm and 350 nm, from which the band-gap energy was evaluated to be 4.03 eV. Furthermore, the fluorescence spectrum was recorded for the prepared samples; the excitation spectrum shows a strong peak at 397 nm, attributed to the ⁴F_{7/2}→⁴G_{11/2} transition, while the emission shows two prominent peaks at 420 nm (⁴G_{7/2}→⁴F_{7/2}) and 440 nm (⁴G_{5/2}→⁴F_{7/2}). The acquired emission results were utilized to confirm the color emission using a chromaticity plot, which found the coordinates to be at (0.1529 0.1040), and the calculated temperature was 3171 K. The as-prepared nanosheets were utilized in detecting latent fingerprints (LFPs) on various non-porous surfaces. The powder-dusting method was used to develop latent fingerprints on various non-porous surfaces, which resulted in detecting all the three ridge patterns. Furthermore, the as-synthesized nanosheets were used to degrade methyl red (MR) dye, the results of which show more than 60% degradation at the 70th minute. It was also found that there was no further degradation after 70 min. All the acquired results suggest the clear potential of the prepared BaLa₂O₄ NSs for use in advanced forensic and photocatalytic applications.

Keywords: BaLa₂O₄ nanomaterials; precipitation method; latent fingerprint detection; dye degradation



Citation: Majani, S.S.; Meghana, S.H.; S.; J., S.; Umesh, S.; Shivamallu, C.; Iqbal, M.; Amachawadi, R.G.; K N, V.; Kollur, S.P. Barium Lanthanum Oxide Nanosheets in Photocatalytic and Forensic Applications: One-Pot Synthesis and Characterization. *Molecules* **2023**, *28*, 7228. <https://doi.org/10.3390/molecules28207228>

Academic Editor: Igor Djerdj

Received: 14 September 2023

Revised: 12 October 2023

Accepted: 13 October 2023

Published: 23 October 2023



Copyright: © 2023 by the authors. Licensee MDPI, Basel, Switzerland. This article is an open access article distributed under the terms and conditions of the Creative Commons Attribution (CC BY) license (<https://creativecommons.org/licenses/by/4.0/>).

1. Introduction

Forensic technology performs a crucial role in the functioning of the criminal justice system, offering fundamental equipment and methodologies for identity evaluation and the interpretation of evidence. The relentless pursuit of justice relies heavily on these technological improvements. Among the numerous forms of forensic evidence, fingerprints have been a cornerstone of investigations for over a century [1,2]. In modern times, visible latent fingerprint detection is at the forefront of investigations, with wide-ranging use in law enforcement, border safety, and biometric authentication [3–7]. Identifying and appraising evidence have emerged as fundamental factors in solving crimes and ensuring that those responsible are brought to justice. In this context, latent fingerprints constitute a crucial aspect. Unlike visible fingerprints, latent prints are hidden from the naked eye and

necessitate specialized strategies for their discovery. This concealed nature is due to the latent prints being composed of the residual oil and sweat left on the ridges of the fingers, which renders latent prints invisible. The traditional method of latent fingerprint detection typically involves the application of fingerprint powder, which conforms to the shape of the residue, as mentioned previously, thereby rendering the latent prints visible. However, this approach is associated with difficulties and may damage the underlying surface. Thus, there has been an escalating call for a non-damaging, less invasive approach to detecting latent fingerprints [8–11].

The relevance and significance of forensic technology in the criminal justice system cannot be overstated. Forensic professionals and investigators depend on its tools to interpret the clues left at the scene by criminals and to establish a transparent chain of evidence. The use of fingerprints in personal identification has deep historical roots, dating back to historic Babylon, where fingerprints were used on clay capsules for commercial enterprise transactions. In the present era, the evaluation of fingerprints achieved prominence as a forensic technology when Sir Francis Galton and Sir Edward Henry advanced the use of fingerprints within the late 19th and early 20th centuries. Since then, fingerprint identification has become a cornerstone of forensic science, criminal investigations, and prison court cases. However, latent fingerprints present a unique challenge. These are impressions left behind by accident, often at crime scenes, on glass, plastic, or metallic surfaces. Unlike visible fingerprints, they are invisible to the human eye. The desire for a more dependable and less destructive technique to uncover these concealed clues has pushed the pursuit of latent fingerprint detection. Historically, the number one technique for latent fingerprint detection has been the technology of fingerprint powder. This method involves dusting the surface containing the latent print with powder, which adheres to the residual oils and sweat, revealing the hidden sample. While powerful, this procedure has inherent barriers. This negative technique can harm or contaminate the underlying surface and may not be applicable in all circumstances. Consequently, there has been a call for alternative, non-invasive methods. Technological improvements in forensics, specifically in latent fingerprint detection, have extensively enriched the criminal justice system, and their utility has extended into broader areas, including regulation enforcement, border safety, and biometric authentication [12–14].

Photocatalytic dye degradation represents a ground-breaking method for the removal of organic harmful dyes from wastewater with the use of the energy of photocatalysts. This approach involves the activation of catalysts that drive the production of reactive oxygen species, which act upon the dye molecules, breaking them into harmless byproducts. Recent advancements in this area have been focused on boosting the efficiency of photocatalysts, generally by harnessing the specific sites of nanomaterials, such as graphene oxide, steel–organic frameworks, and quantum dots, as highlighted in numerous studies. These advanced substances provide significantly increased light absorption capabilities, ultimately leading to greener and more eco-friendly dye degradation. Additionally, researchers have delved into modifying photocatalysts to target unique dye types and optimizing response times to achieve advanced overall performance. These collective efforts have fantastic promise for a powerful and environmentally friendly remedy for water resources contaminated with dyes [15–17].

Photocatalytic dye degradation is increasingly recognized as an environmentally friendly solution to address the widespread issue of dye pollution in water. The process relies on using photocatalysts, materials that can potentially use light energy and convert it into chemical energy (ROS). These produced ROS are very potent and play an essential role in degrading organic compounds through chemical reactions. ROS efficiently degrade the organic dyes by breaking them into simple, non-toxic compounds.

One of the primary areas of research in this discipline has been enhancing photocatalysts' overall performance. This objective has led to the exploration of diverse nanomaterials, which display properties that may enhance the performance of photocatalysis. Notably, metal oxides have emerged as a promising candidate due to their excellent tunable surface

area and exceptional electric conductivity. These properties enable them to be ideal photocatalyst materials, enhancing their stability and catalytic nature. Similarly, graphene and quantum dots have shown fantastic capability in improving photocatalytic performance. Metal oxide frameworks (MOFs) possess a porous structure that enables dye adsorption, while quantum dots showcase outstanding light-absorbing capabilities, allowing for better energy conversion in photocatalytic reactions.

Using nanomaterials in photocatalysis complements the method's efficiency and contributes to its environmental sustainability. By increasing the surface region for catalysis and enhancing light absorption, these materials reduce the amount of the photocatalyst required for effective dye degradation. This translates to lower material use, decreased energy expenditure, and a more environmentally friendly technique for wastewater remediation. Furthermore, researchers have been eager to customize photocatalysts to target dyes. Organic dyes are available in myriad structures and compositions, each one requiring a tailor-made approach for green degradation. Through the amendment of photocatalysts, scientists can fine-tune their catalytic properties to suit the dye contaminants' traits better. This degree of specificity guarantees that the photocatalytic system stays powerful across a wide range of dye pollution.

In addition to customizing photocatalysts, optimizing the response times has been a focus of recent studies. Researchers are diligently working to identify the ideal parameters for photocatalytic dye degradation, including the awareness of photocatalysts, the duration of exposure to light, and the pH of the solution. These efforts aim to maximize the method's performance while minimizing energy consumption and ensuring constant outcomes in diverse environmental conditions.

Luminescent materials are one of the most promising techniques for detecting latent fingerprints [11]. Luminescent substances emit light when exposed to a specific sort of energy, including ultraviolet light or X-rays. Using luminescent materials makes it viable to enhance the identification of latent fingerprints and detect even faint or invisible prints. Several luminescent materials, which include metal oxides (MOs), quantum dots (QDs), and primarily lanthanide-based substances, have been studied for use in latent fingerprint detection [18–22]. Among these luminescent materials, primarily lanthanide-based materials have shown first-rate potential in latent fingerprint detection because of their photophysical properties [23]. Lanthanide ions have electronic transitions with sharp and narrow emission bands, which permits great sensitivity and selectivity in detecting latent fingerprints.

Nanomaterials involving Barium and Lanthanum have recently garnered interest for their potential applicability in the discipline of forensics. These nanomaterials have precise properties that make them appropriate for forensic applications, including fingerprint detection and analysis. Nanomaterials prepared with these factors are recognized for their chemical stability, which permits them to keep their physical and chemical properties even after exposure to diverse environmental situations. This stability makes them perfect for fingerprint detection, wherein the nanomaterials can be applied to surfaces to expose latent fingerprints that are not visible to the naked eye. Moreover, the involvement of a lanthanide (Lanthanum) makes these nanomaterials exhibit strong luminescence properties, which can be exploited in forensic evaluation. These properties have made them a promising candidate for forensic applications [24,25]. Further studies are warranted to discover these nanomaterials' capabilities in the field of forensics.

In the present study, BaLa₂O₄ NSs were synthesized using the co-precipitation method. The prepared sample was subjected to various techniques to characterize its structural, surface morphology, and luminescent information. Furthermore, latent fingerprint visualization was conducted using the powder-dusting method to assess the potential of the prepared NPs for use in advanced forensic applications.

2. Results and Discussion

2.1. PXRD Analysis

The structural analysis of nanomaterials plays a pivotal role in figuring out their potential for application in the fields of forensics and catalysis. In forensics, the structures of nanomaterials, including their high surface area and tunable reactivity, allow them to be employed in detecting and evaluating trace evidence, providing desirable sensitivity and specificity in crime scene investigations. Moreover, their potential as catalysts, often derived from properly defined nanostructures, makes them precious in catalysis programs, facilitating more efficient and sustainable chemical reactions. The capacity to tailor nanomaterial systems allows for precision in each forensic and catalytic context, making them essential tools in these domains.

PXRD analysis was conducted on the as-synthesized BaLa_2O_4 NSs to determine their crystallite structure and phase identification, essential for understanding their properties and potential applications. Figure 1 depicts the PXRD profile, which displays similarity to the data retrieved from the Materials Project for BaLa_2O_4 (mp-752656) from database version v2022.10.28 with space group Pnma and the orthorhombic phase of the parameters $a = 3.70 \text{ \AA}$, $b = 10.67 \text{ \AA}$, and $c = 12.66 \text{ \AA}$ [26]. Furthermore, the as-obtained results were analyzed to evaluate the crystallite size of the sample using the Scherrer equation [27],

$$D = \frac{k\lambda}{\beta \cos\theta}$$

where D , k , λ , β , and θ represent the crystallite size, shape factor of 0.9, wavelength of the X-rays used, full width at half maximum of the profile peaks, and diffracting angle, respectively, and D was found to be 27 nm.

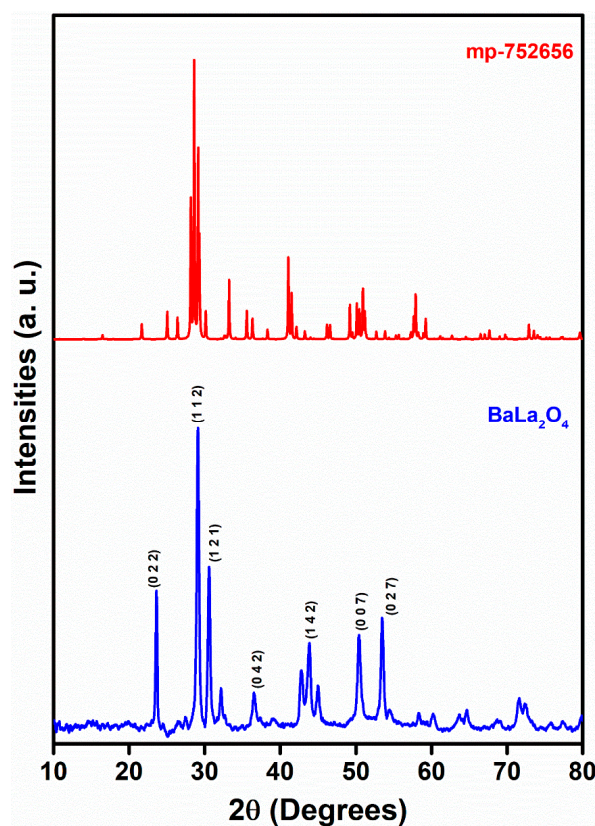


Figure 1. XRD profile of prepared BaLa_2O_4 NSs assigned with hkl values from mp-752656.

2.2. Morphology

Morphological evaluation of nanomaterials is pivotal in assessing their suitability for forensic and catalytic applications. The unique structural traits of nanomaterials, their size, shape, and surface area, are important in determining their effectiveness in numerous domains. In forensics, the distinct morphological functions of nanomaterials enable their usage in fingerprint analysis and evidence detection. Their large surface-to-area ratio enhances their sensitivity, and tailored shapes and compositions provide numerous applications. In catalysis, the morphology governs the catalytic ability of the nanomaterial, influencing its response kinetics and selectivity. Nanomaterials' tunable structures allow them to have a role as catalysts in various applications, which are important in developing sustainable techniques. This synergy between morphological analysis and nanomaterials' properties underscores their ability to advance forensic and catalytic technology.

Hence, the prepared sample was subjected to FESEM and SEM for surface morphology and EDAX mapping. Figure 2 delineates an irregular stack structure at different magnifications, with regions layered on top of one another. Furthermore, the elemental composition is authenticated by Figure 3, the EDAX spectrum, showing the high purity of the precursors' elements. Figure 4 reveals the mapping of Barium (Ba L), Lanthanum (La L), and Oxygen (O K) in the selected 100 μm area of the as-synthesized sample.

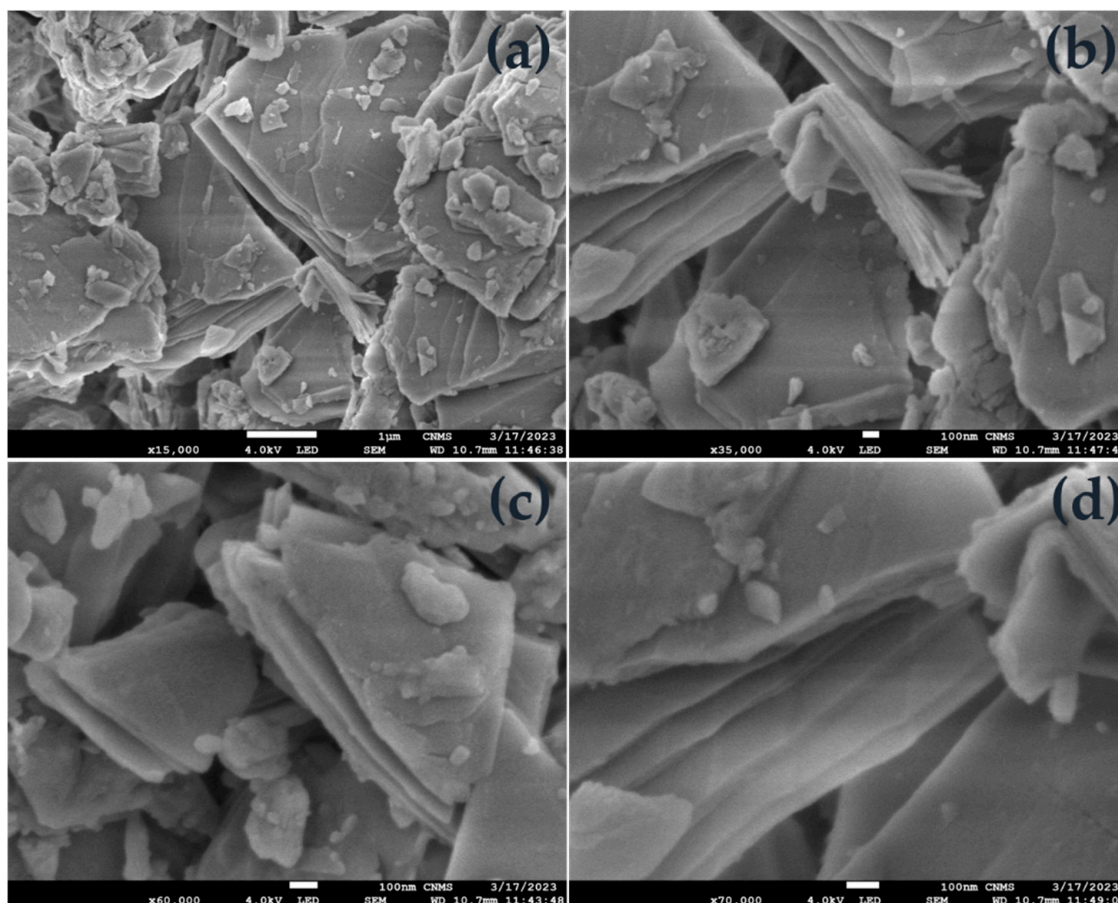


Figure 2. FESEM micrographs with different resolutions ((a) 1 μm , and (b–d) 100 nm) of the as-prepared BaLa₂O₄ NSs.

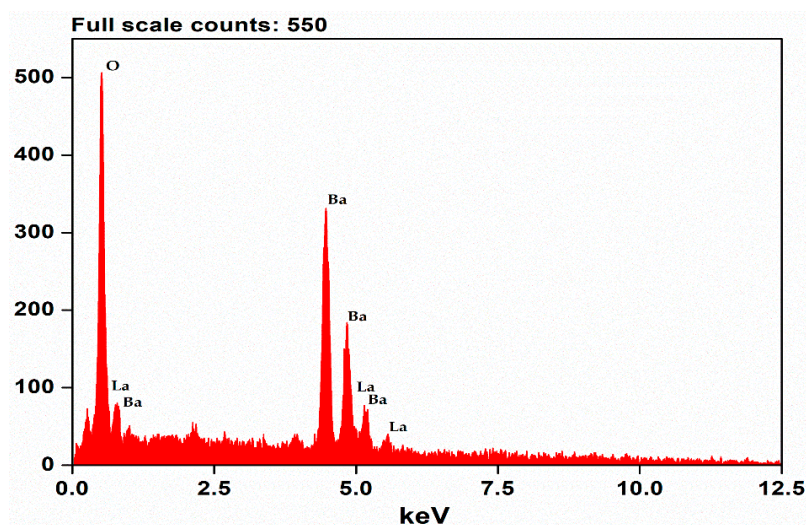


Figure 3. EDAX spectrum showing high purity of precursor elements.

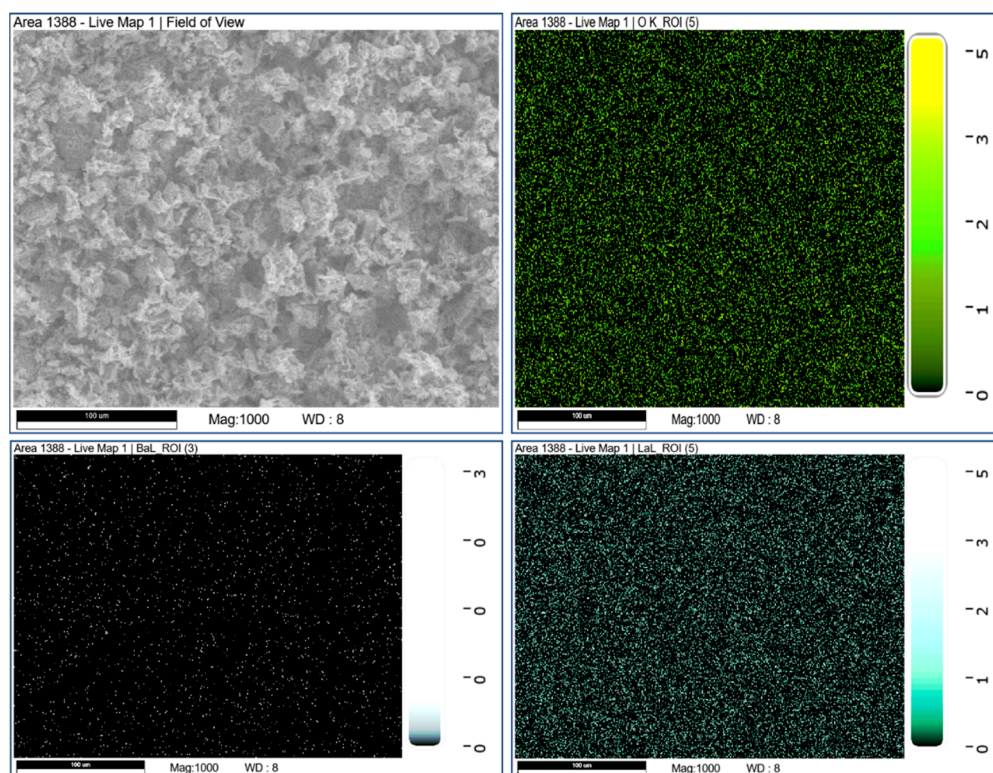


Figure 4. Mapping of precursor elements over a selected area using EDAX analysis.

2.3. DRS Studies

The inspection of the optical properties of nanomaterials plays a pivotal role in endorsing them as compelling candidates in both forensics and catalysis. Nanomaterials are engineered on the nanoscale, having properties that set them aside from bulk materials. These unique features make them useful in diverse applications. In forensics, the optical properties of nanomaterials are harnessed for their capability to enhance the detection and evaluation of evidence. Nanoparticles may be tailor-made to exhibit optical properties, including fluorescence. This allows them to behave as molecular tags or labels for evidence, making it less complicated to identify latent fingerprints, organic materials, or different strains at crime scenes. For example, nanomaterials with tunable fluorescence properties can bind to blood, semen, or other physical fluids, illuminating crime scene

evidence beneath specialized light sources. This allows for quicker and more correct forensic evaluation.

Moreover, nanomaterials have emerged as having potential applications as catalysts due to their large surface-to-area ratio and capability to function as catalysts in various chemical reactions. Their optical properties are instrumental in tracking and controlling catalytic reactions. Researchers can use real-time insights into reaction kinetics and pathways by incorporating nanomaterials with precise optical signatures into catalytic procedures. This not only effectively enhances the performance of catalytic reactions, it also affords a tool for information and optimizing complex chemical methods.

A diffused reflectance (DR) spectrum ranging between 200 nm and 600 nm was observed, as depicted in Figure 5a, showing two bands centered at 223 nm and 310 nm, further appraised for the calculation of the energy band gap (E_g) using the Kubelka–Munk function, given as [28]

$$F(R_\infty) = \frac{(1 - R_\infty)^2}{2R_\infty}$$

$$h\nu = \frac{1240}{\lambda}$$

where $h\nu$ is the photon energy, $F(R_\infty)$; R_∞ is the reflection co-efficient; and λ is the wavelength absorbed. The estimated E_g of the as-synthesized BaLa₂O₄ NSs was 4.03 eV, as depicted in Figure 5b. Furthermore, the evaluated E_g was utilized to find the refractive index of the prepared sample using the relation [29]

$$\frac{n^2 - 1}{n^2 + 1} = 1 - \frac{\sqrt{E_g}}{20}$$

where n , the refractive index, was found to be 0.73.

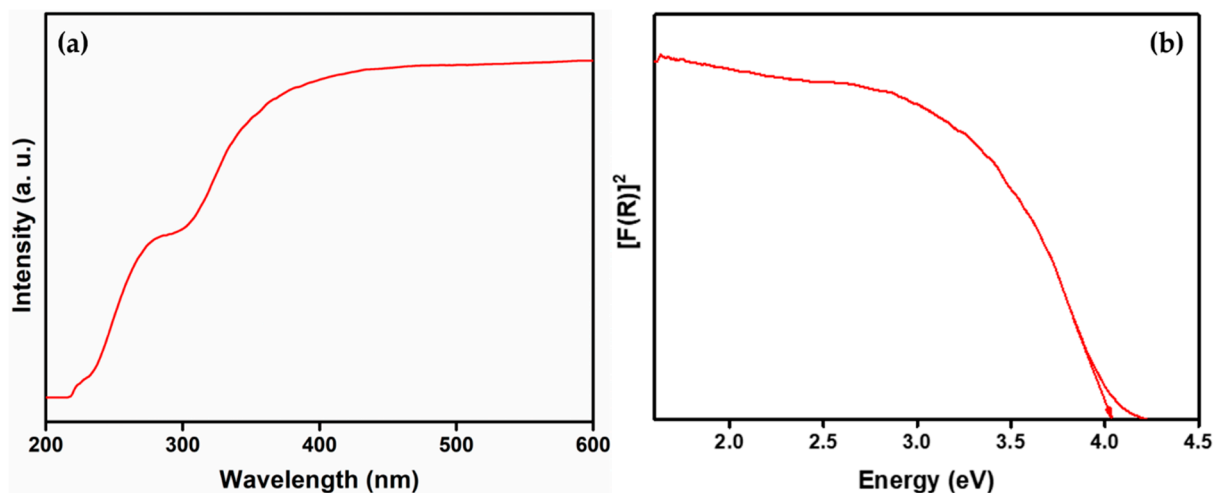


Figure 5. DR spectrum (a) and band-gap calculation (b) of the prepared BaLa₂O₄ NSs.

2.4. Fluorescence Studies

The prepared sample was studied for its fluorescence properties since Lanthanum (a lanthanide group element with active f-transitions) was involved. Figure 6a shows the excitation spectrum of the BaLa₂O₄ NSs at the 440 nm emission wavelength, and the characteristic peak at 397 nm was observed for an effective $^4F_{7/2} \rightarrow ^4G_{11/2}$ transition. Furthermore, the observed excitation was utilized to record the emission spectrum, depicted in Figure 6b. The results obtained show two prominent peaks at 420 nm ($^4G_{7/2} \rightarrow ^4F_{7/2}$) and 440 nm ($^4G_{5/2} \rightarrow ^4F_{7/2}$) [30,31].

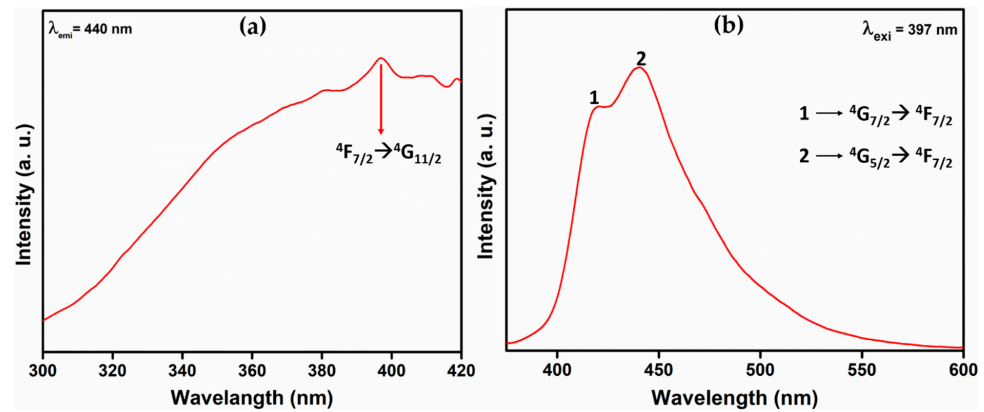


Figure 6. (a) Excitation spectrum at $\lambda_{\text{emi}} = 440$ nm, and (b) emission spectrum at $\lambda_{\text{exi}} = 397$ nm of the prepared BaLa_2O_4 NSs.

2.5. Chromaticity Analysis

In assessing its aptness as a luminescent material, the fabricated BaLa_2O_4 NSs were subjected to a color emissivity test using the Commission International de l'Éclairage (CIE-1931) [27,32]. Figure 7a,b show the CIE chromaticity diagram and the corresponding CCT diagrams of the as-synthesized BaLa_2O_4 NSs obtained using emission studies at 397 nm excitation. The calculation of the CCT value from the obtained co-ordinates (0.1529, 0.1040) was performed using the McCamy empirical formula, as in [33],

$$\text{CCT} = -499n^3 + 352n^2 - 6823.3n + 5520.33$$

$$n = \frac{x - x_e}{y - y_e}$$

where (x_e, y_e) are the color epicenter and (x, y) are the obtained CIE coordinates, and the CCT value was found to be 3171 K. Further, the percentage color purity for the obtained coordinates was evaluated utilizing the following relation [34]:

$$\text{CP} = \frac{\sqrt{(x_s - x_i)^2 + (y_s - y_i)^2}}{\sqrt{(x_d - x_i)^2 + (y_d - y_i)^2}} \times 100\%$$

where (x_s, y_s) are the coordinates of the samples, (x_d, y_d) are the dominating wavelengths, and (x_i, y_i) are the illuminating coordinates. The obtained results show a 91% blue emission.

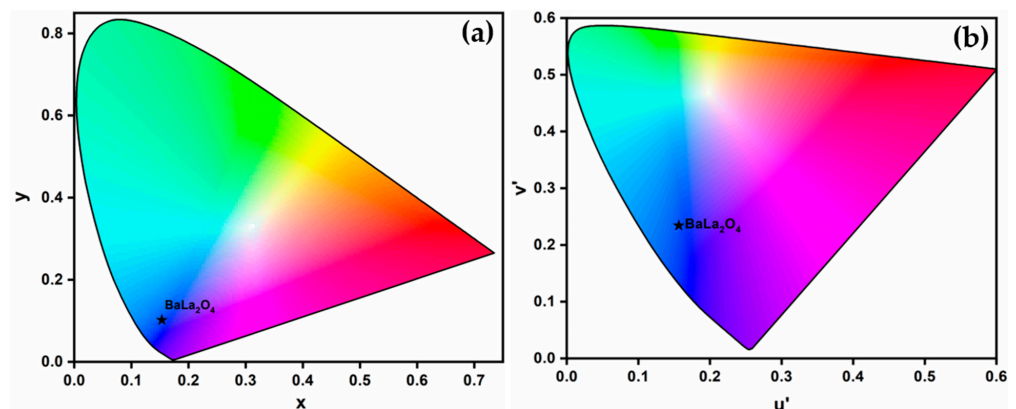


Figure 7. CIE (a) and CCT (b) plot using emission at $\lambda_{\text{exi}} = 397$ nm of the prepared BaLa_2O_4 NSs. ★ represents the point of maximum emission.

2.6. Latent Fingerprints (LFPs) Visualization

Latent fingerprint detection through powder dusting is a fundamental and widely used method in forensic science. This approach reveals hidden fingerprints not seen by the naked eye. It is conducted using a fingerprint powder on surfaces where latent prints are suspected. The powder adheres to the residual oils and sweat left at the ridges of the fingerprints, making them stand out from the surface. The method involves careful usage of the powder, which is then lightly brushed or dusted onto the surface. The excess powder is cautiously removed, leaving a clear and detailed identification of the latent fingerprint. This method is critical for crime scene investigations, permitting forensic professionals to acquire and analyze evidence that may be essential in solving crimes and bringing perpetrators to justice. The simplicity and effectiveness of powder dusting make it an important device within the forensics toolkit. Different ridge pattern identification techniques have seen increased interest in advanced forensic applications [35,36]. Generally, ridge patterns are recognized by type-I (whorls, loops, eyes), type-II (ridge ends, bifurcations, bridges, hooks), and type-III (sweat pores) characteristics, using various techniques [20,37–39]. One such traditional technique, the powder-dusting method, was employed for the as-synthesized BaLa_2O_4 NSs to develop latent fingerprints (LFPs) on different non-porous surfaces (glass, aluminium foil, and stainless steel). Figure 8 depicts the upfront hindrance-free ridge pattern detections on glass (A), aluminium (B), and stainless steel (C), captured using a Sony DSC-W690 Cyber-shot camera under white light. The acquired results show that the prepared samples detect type-I, type-II, and even type-III patterns without any background hindrance. The outcomes recommend the as-synthesized BaLa_2O_4 NSs for their potential use in advanced forensics applications.

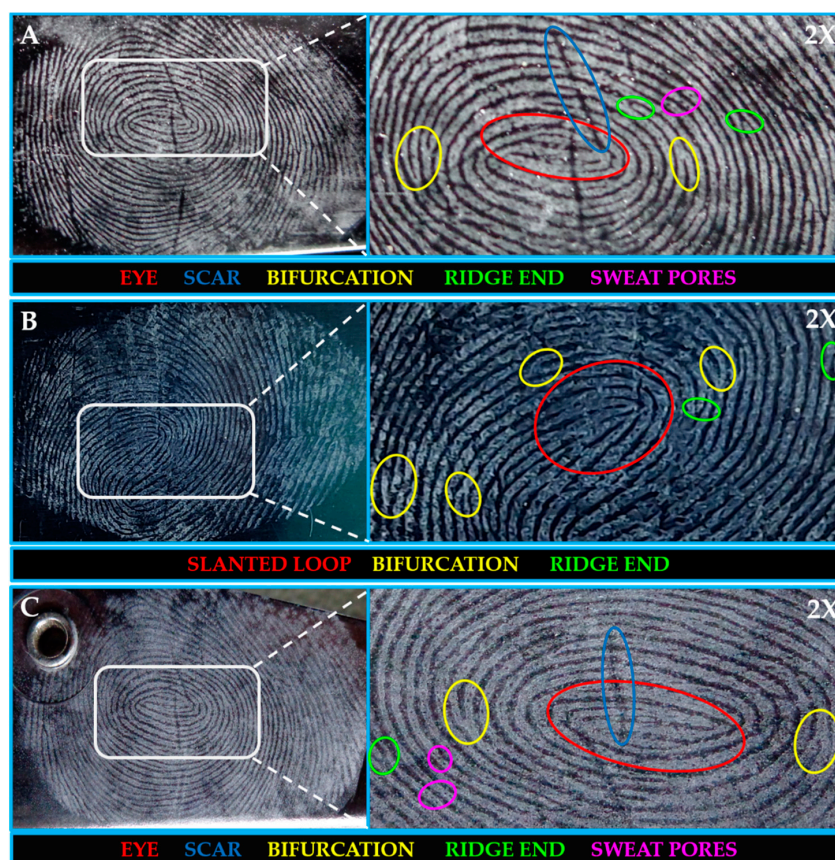


Figure 8. Latent fingerprints developed using powder dusting over glass (A), aluminium (B), and stainless steel (C). The detection was observed at 2× magnification of the captured images.

2.7. MR Degradation by BaLa₂O₄ NSs

Photocatalysis is an innovative and environmentally friendly method for degrading organic dyes. This process harnesses the power of light and a photocatalyst, typically a semiconductor material like a simple metal oxide, to break down organic compounds into harmless byproducts. When exposed to light, the photocatalyst generates electron-hole pairs, initiating redox reactions that oxidize and degrade the organic dyes. The critical advantage of photocatalysis is its ability to efficiently degrade a wide range of organic dyes, even those that are challenging to treat using conventional methods. It is a sustainable approach, as it does not rely on harsh chemicals or produce harmful residues. Moreover, it can be applied in diverse settings, from wastewater treatment to air purification. Photocatalysis represents a promising solution for addressing environmental pollution and offers a cleaner, more sustainable pathway for tackling the challenges associated with organic dye degradation.

The photocatalytic dye degradation of MR dye was performed using the prepared BaLa₂O₄ NSs. A mass of 60 mg of the prepared photocatalyst was added to 100 mL of 10 ppm dye solution and an adsorption equilibrium was attained on stirring it vigorously in the dark for 20 min. After adding the photocatalyst, 3 mL of the solution was withdrawn every 10 min and centrifuged to study the absorption, as depicted in Figure 9a. The location of the absorption band of Methyl Red, at 430 nm, was found to be unaltered, and the peak decreased as a function of time. The degradation percentage was calculated using the relation [40]

$$\% \text{ Degradation} = \left[\frac{C_0 - C}{C_0} \right] \times 100$$

where C_0 and C are the initial and current concentrations. The results show that the percentage of degradation of the MR dye was 24% (10 min), 34% (20 min), 50% (40 min), and 62% (70 min), as depicted in Figure 9b. Also, it was found that there was no further degradation after 70 min.

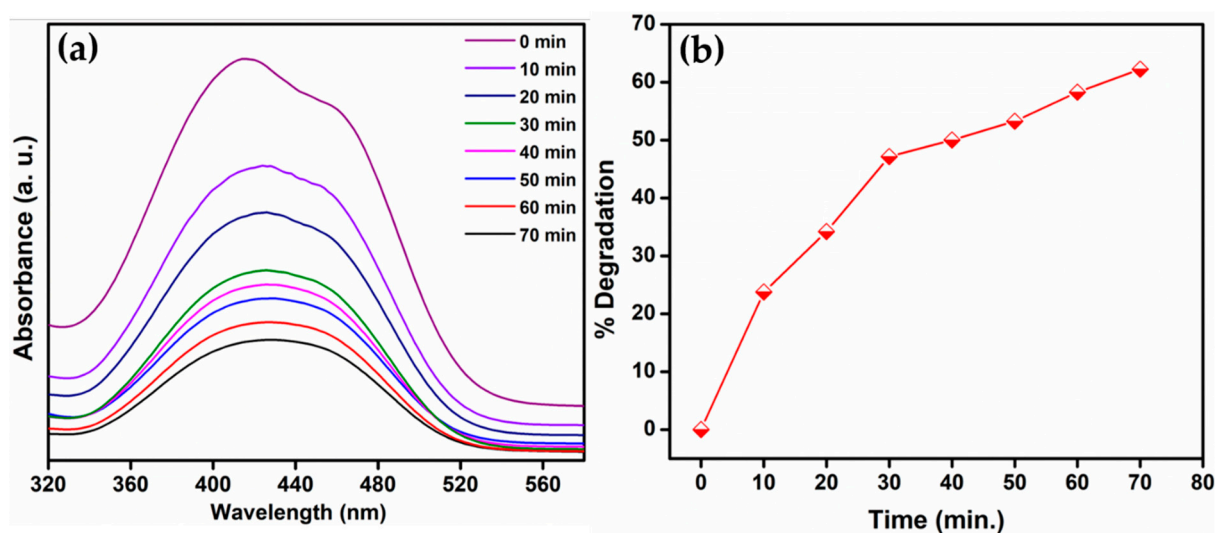


Figure 9. Photocatalytic performance of BaLa₂O₄ NSs against MR dye. (a) Absorption spectrum of as-prepared photocatalyst; (b) graph representing the degradation of MR dye at various concentrations.

3. Experimental

3.1. Materials and Methods

Barium nitrate (Ba(NO₃)₂) and lanthanum nitrate (La(NO₃)₃) were purchased from Sigma (Carlsbad, CA, USA). Synthetic methyl red (MR) (C₁₅H₁₅N₃O₂), available in the laboratory, was used in the photocatalytic dye degradation. A high-resolution Bruker powder X-ray diffractometer (Karlsruhe, Germany) was used to study the phase dynamics of the prepared sample. A JOEL JSM-7100F FESEM and EVO MA 15 (Carl Zeiss, Schleswig-

Holstein S-H, Germany) were used to determine the surface morphology and confirm the elemental composition of the prepared sample. The absorption band was produced using a UV-3200 (Lab India, Mumbai, India) double-beam UV–Visible spectrophotometer for band-gap analysis. A SHIMADZU fluorescence spectrophotometer was used for photoluminescence analysis of the prepared samples. A Rotek UV chamber was used to detect latent fingerprint designs on various surfaces.

3.2. Synthesis of $BaLa_2O_4$ Nanosheets

A one-pot co-precipitation method (Figure 10) was utilized to synthesize the $BaLa_2O_4$ NSs. Stoichiometric amounts of $Ba(NO_3)_2$ (2.6133 g) and $La(NO_3)_3$ (4.3301 g) were measured and transferred to a 100 mL round-bottom flask. This was then completely dissolved in 25 mL of water, giving a homogeneous mixture. The mixture obtained was kept on a hot stirrer for about 7 to 8 h until the precipitation was complete. Furthermore, the precipitate was centrifuged at room temperature at 900 rpm for about 20 min to separate it from the solvent. The precipitate was air-dried at 70 °C in an oven and further calcinated at 700 °C for further characterization. The yield was estimated to be about 83% (5.7630 g).

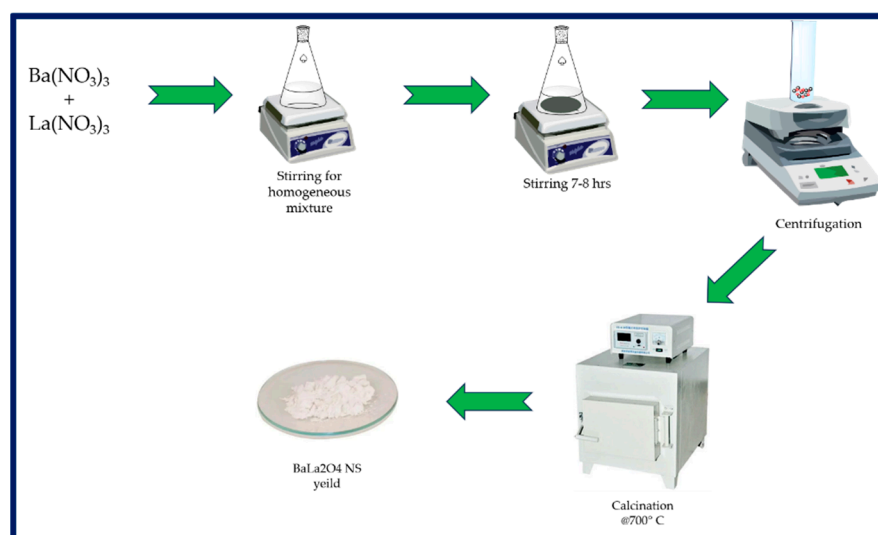


Figure 10. Flowchart representing the one-pot synthesis of $BaLa_2O_4$ NSs.

3.3. Photocatalytic Degradation Activity

The synthesized $BaLa_2O_4$ nanosheets' (NSs) overall catalytic performance was investigated using synthetic MR dye as the model pollutant. Initially, 100 mL of solution containing 20 parts per million (ppm) of MR dye was prepared. To establish the desorption equilibrium between the photocatalyst and the dye, the prepared solution, containing the dye and photocatalyst, underwent lively stirring in the dark for 20 min. The prepared samples featured a sizeable percentage of La_2O_3 , recognized for its first-rate photocatalytic ability in degrading synthetic dyes [24,25]. Consequently, after adding the photocatalyst to the MR dye solution, absorption measurements were taken at the 0 min mark to gauge the initial absorbance. Subsequently, at 10 min intervals, samples were extracted from the solution on the stirrer. These samples were then subjected to centrifugation to remove any coagulated catalyst, ensuring that the analysis was centered totally on the outcomes of the photocatalyst. The absorption traits of the solution were tested at these time points. This systematic technique allowed for a complete evaluation of the catalytic performance of the $BaLa_2O_4$ nanosheets in degrading the MR dye, with absorption measurements at different time points providing valuable insights into the degradation kinetics and performance of the photocatalytic technique.

4. Conclusions

In summary, a simple co-precipitation method was utilized to fabricate BaLa₂O₄ NSs. The prepared sample was investigated using PXRD, FESEM, UV, and a fluorescence spectrophotometer. The structural results show that the prepared sample matched the data retrieved from the Materials Project database, mp-752656, having an orthorhombic phase. Irregular sheet shapes stacked on top of one another in a layer-like morphology were observed from the morphology studies. The distribution of the precursor elements in the prepared sample was confirmed from EDAX mapping analysis. DRS studies depict a strong peak at 310 nm, from which the calculated energy band gap and refractive index were 4.03 eV and 0.73, respectively. The excitation spectrum shows a strong excitation at 397 nm (⁴F_{7/2} → ⁴G_{11/2}) with the 440 nm emission maintained, alongside an emission spectrum depicting two prominent peaks at 420 nm (⁴G_{7/2} → ⁴F_{7/2}) and 440 nm (⁴G_{5/2} → ⁴F_{7/2}), maintained at 397 nm excitation. Further, the CIE-1931 diagram confirming the color emission with coordinates (0.1529, 0.10401) was utilized to calculate the CCT, which was found to be 3171 K. The obtained coordinates were utilized to evaluate the CP%, the result of which was a purity of 91%. The as-prepared nanosheets were used with the powder-dusting method to detect latent fingerprints developed on various non-porous surfaces (glass, aluminium, and stainless steel). The obtained results depict the detection of up to a type-III level ridge pattern. Furthermore, an effective dye degradation against methyl red was conducted by making use of the synthesized BaLa₂O₄ NSs; up to 62.23% of the methyl red was degraded, with no further degradation after 70 min. All the acquired results suggest the prepared BaLa₂O₄ NSs as a potent candidate in advanced forensic and photocatalytic applications.

Author Contributions: S.S.M. and M.: conceptualization, methodology, software. S.S.M., S.S.H. and S.J.: data curation, writing—original draft preparation. S.U., C.S. and M.I.: visualization, investigation. R.G.A., V.K.N. and S.P.K.: supervision. R.G.A., C.S. and M.I.: software, validation. V.K.N. and S.P.K.: writing—reviewing and editing. All authors have read and agreed to the published version of the manuscript.

Funding: The authors extend their appreciation to the “Researchers Supporting Project number (RSPD2023R734), King Saud University, Riyadh, Saudi Arabia” for financial support.

Institutional Review Board Statement: Not applicable.

Informed Consent Statement: Not applicable.

Data Availability Statement: Data is contained within the article.

Acknowledgments: All the authors sincerely thank Amrita Vishwa Vidyapeetham, Mysuru, for infrastructural support. The authors extend their appreciation to the “Researchers Supporting Project number (RSPD2023R734), King Saud University, Riyadh, Saudi Arabia” for financial support.

Conflicts of Interest: The authors declare no conflict of interest.

Sample Availability: Samples of the compounds are available from the authors.

References

1. Majani, S.S.; Gowda, B.G.; Prema, R.; Usha, V.; Shivamallu, C.; Iqbal, M.; Amachawadi, R.G.; Venkatachalaiah, K.; Kollur, S.P. Dysprosium doped BaMgO₂ nanopowders as highly luminescent materials: Preparation, characterization, and forensic application. *Inorg. Chem. Commun.* **2023**, *155*, 111133. [[CrossRef](#)]
2. Majani, S.S.; Basavaraj, R.; Venkatachalaiah, K.; Kollur, S.P.; Chandrasekhar, T. Versatile deep red-emitting SrCeO₃: Eu³⁺ nanopowders for display devices and advanced forensic applications. *J. Solid State Chem.* **2023**, *329*, 124360. [[CrossRef](#)]
3. Yang, K.; Tang, H.; Jiao, Y.; Gao, L.; Zhang, M.; Qin, J.; Li, W.; Lu, S.; He, Y. An AIE-active orange-emitting cationic iridium(III) complex for latent fingerprints detection via a simple powder dusting method. *J. Lumin.* **2023**, *257*, 119721. [[CrossRef](#)]
4. Prabakaran, E.; Pillay, K. Nanomaterials for latent fingerprint detection: A review. *J. Mater. Res. Technol.* **2021**, *12*, 1856–1885. [[CrossRef](#)]
5. Singla, N.; Kaur, M.; Sofat, S. Automated latent fingerprint identification system: A review. *Forensic Sci. Int.* **2020**, *309*, 110187. [[CrossRef](#)]

6. Pushpendra; Suryawanshi, I.; Kalia, R.; Kunchala, R.K.; Mudavath, S.L.; Naidu, B.S. Detection of latent fingerprints using luminescent $\text{Gd}_{0.9}\text{Eu}_{0.05}\text{PO}_4$ nanorods. *J. Rare Earths* **2021**, *40*, 572–578. [[CrossRef](#)]
7. Trabelsi, H.; Akl, M.; Akl, S.H. Ultrasound assisted Eu^{3+} -doped strontium titanate nanophosphors: Labeling agent useful for visualization of latent fingerprints. *Powder Technol.* **2021**, *384*, 70–81. [[CrossRef](#)]
8. Yuan, C.; Li, M.; Wang, M.; Zhang, L. Cationic dye-diatomite composites: Novel dusting powders for developing latent fingerprints. *Dye. Pigment.* **2018**, *153*, 18–25. [[CrossRef](#)]
9. Ashwini, K.; Premkumar, H.; Darshan, G.; Prasad, B.D.; Nagabhushana, H.; Sharma, S.; Prashantha, S. Dysprosium doped strontium aluminate dusting powder: Sweat pores visualization and white LED component. *Inorg. Chem. Commun.* **2021**, *134*, 109028. [[CrossRef](#)]
10. Niu, X.; Song, T.; Xiong, H. Large scale synthesis of red emissive carbon dots powder by solid-state reaction for fingerprint identification. *Chin. Chem. Lett.* **2021**, *32*, 1953–1956. [[CrossRef](#)]
11. Errington, B.; Lawson, G.; Lewis, S.W.; Smith, G.D. Micronised Egyptian blue pigment: A novel near-infrared luminescent fingerprint dusting powder. *Dye. Pigment.* **2016**, *132*, 310–315. [[CrossRef](#)]
12. Yuan, C.; Wang, M.; Li, M. Design and synthesis of silica- and silicate-based materials, and their application in the development and analysis of latent fingerprints. *TrAC Trends Anal. Chem.* **2023**, *167*, 117278. [[CrossRef](#)]
13. Gomes, F.M.; de Pereira, C.M.P.; Mariotti, K.d.C.; Pereira, T.M.; dos Santos, N.A.; Romão, W. Study of latent fingerprints—A review. *Forensic Chem.* **2023**, *35*, 100525. [[CrossRef](#)]
14. Sun, L.; Zhang, Y.; Lv, X.-S.; Li, H.-D. A luminescent Eu-based MOFs material for the sensitive detection of nitro explosives and development of fingerprint. *Inorg. Chem. Commun.* **2023**, *156*, 111267. [[CrossRef](#)]
15. Dihom, H.R.; Al-Shaibani, M.M.; Mohamed, R.M.S.R.; Al-Gheethi, A.A.; Sharma, A.; Bin Khamidun, M.H. Photocatalytic degradation of disperse azo dyes in textile wastewater using green zinc oxide nanoparticles synthesized in plant extract: A critical review. *J. Water Process Eng.* **2022**, *47*, 102705. [[CrossRef](#)]
16. Elbadawy, H.A.; Elhusseiny, A.F.; Hussein, S.M.; Sadik, W.A. Sustainable and energy-efficient photocatalytic degradation of textile dye assisted by ecofriendly synthesized silver nanoparticles. *Sci. Rep.* **2023**, *13*, 2302. [[CrossRef](#)]
17. Lal, M.; Sharma, P.; Singh, L.; Ram, C. Photocatalytic degradation of hazardous Rhodamine B dye using sol-gel mediated ultrasonic hydrothermal synthesized of ZnO nanoparticles. *Results Eng.* **2023**, *17*, 100890. [[CrossRef](#)]
18. Renuka, L.; Anantharaju, K.; Gurushantha, K.; Nagabhushana, H.; Vidya, Y.; Suresh, C.; Sennappan, M. Phase-transformation synthesis of Li codoped ZrO_2 : Eu^{3+} nanomaterials: Characterization, photocatalytic, luminescent behavior and latent fingerprint development. *Ceram. Int.* **2021**, *47 Pt B*, 10332–10345. [[CrossRef](#)]
19. Darshan, G.; Prasad, B.D.; Premkumar, H.; Sharma, S.; Kiran, K.; Nagabhushana, H. 20—Fluorescent quantum dots as labeling agents for the effective detection of latent fingerprints on various surfaces. In *Quantum Dots*; Woodhead Publishing Series in Electronic and Optical Materials; Kalyani, N.T., Dhoble, S.J., Domanska, M.M., Vengadaesvaran, B., Nagabhushana, H., Arof, A.K., Eds.; Woodhead Publishing: Sawston, UK, 2023; pp. 539–574. [[CrossRef](#)]
20. Zhou, H.; Chen, H.; Ma, R.; Li, X.; Du, X.; Zhang, M. Use of conductive Ti_2O_3 nanoparticles for optical and electrochemical imaging of latent fingerprints on various substrates. *J. Electroanal. Chem.* **2023**, *936*, 117387. [[CrossRef](#)]
21. Bandi, R.; Kannikanti, H.G.; Dadigala, R.; Gangapuram, B.R.; Vaidya, J.R.; Guttena, V. One step synthesis of hydrophobic carbon dots powder with solid state emission and application in rapid visualization of latent fingerprints. *Opt. Mater.* **2020**, *109*, 110349. [[CrossRef](#)]
22. Girisha, H.; Krushna, B.; Prasad, B.P.; Sharma, S.; Srikanth, C.; Kumar, J.B.P.; Nagabhushana, H. A novel single phase $\text{La}_2\text{CaZnO}_5$: Dy^{3+} phosphor for potential applications in WLED's, latent fingerprint and cheiloscopy. *J. Lumin.* **2023**, *255*, 119539. [[CrossRef](#)]
23. Pavitra, E.; Raju, G.S.R.; Park, J.Y.; Hussain, S.K.; Chodankar, N.R.; Rao, G.M.; Han, Y.-K.; Huh, Y.S. An efficient far-red emitting $\text{Ba}_2\text{LaNbO}_6$: Mn^{4+} nanophosphor for forensic latent fingerprint detection and horticulture lighting applications. *Ceram. Int.* **2020**, *46*, 9802–9809. [[CrossRef](#)]
24. Park, J.Y.; Jang, K.W.; Yang, H.K. Development of red-emitting $\text{Ba}_2\text{LaSbO}_6$: Mn^{4+} phosphors for latent fingerprint detection. *Ceram. Int.* **2021**, *47*, 19496–19504. [[CrossRef](#)]
25. Sehwat, P.; Khatkar, A.; Boora, P.; Kumar, M.; Singh, S.; Malik, R.K.; Khatkar, S.P.; Taxak, V.B. Fabrication of single-phase BaLaAlO_4 : Dy^{3+} nanophosphors by combustion synthesis. *Mater. Manuf. Process.* **2020**, *35*, 1259–1267. [[CrossRef](#)]
26. Ikram, M.; Abid, N.; Haider, A.; Ul-Hamid, A.; Haider, J.; Shahzadi, A.; Nabgan, W.; Goumri-Said, S.; Butt, A.R.; Benali Kanoun, M. Toward efficient dye degradation and the bactericidal behavior of Mo-doped La_2O_3 nanostructures. *Nanoscale Adv.* **2022**, *4*, 926–942. [[CrossRef](#)] [[PubMed](#)]
27. Yamagata, N.; Igarashi, K.; Saitoh, H.; Okazaki, S. Preparation of a Voluminous Composite Oxide of BaLa_2O_4 and Its Catalytic Performance for the Oxidative Coupling of Methane. *Bull. Chem. Soc. Jpn.* **1993**, *66*, 1799–1806. [[CrossRef](#)]
28. The Materials Project. *Materials Data on BaLa_2O_4 by Materials Project*; U.S. Department of Energy Office of Scientific and Technical Information: Oak Ridge, TN, USA, 2020.
29. Basavaraj, R.B.; Navami, D.; Deepthi, N.; Venkataravanappa, M.; Lokesh, R.; Kumar, K.S.; Sreelakshmi, T.K. Novel orange-red emitting Pr^{3+} doped CeO_2 nanopowders for white light emitting diode applications. *Inorg. Chem. Commun.* **2020**, *120*, 108164. [[CrossRef](#)]

30. Sushma, K.C.; Basavaraj, R.; Aarti, D.; Reddy, M.M.; Nagaraju, G.; Rudresha, M.; Kumar, H.S.; Venkatachalaiah, K. Efficient red-emitting SrZrO₃:Eu³⁺ phosphor superstructures for display device applications. *J. Mol. Struct.* **2023**, *1283*, 135192. [[CrossRef](#)]
31. Sonika; Han, S.-D.; Khatkar, S.; Kumar, M.; Taxak, V. Sol-gel synthesis, characterization and luminescent properties of Tb³⁺ doped MLa₂O₄ (M=Sr or Ba) nanophosphors. *Mater. Sci. Eng. B* **2013**, *178*, 1436–1442. [[CrossRef](#)]
32. Mari, B.; Singh, K.; Sahal, M.; Khatkar, S.; Taxak, V.; Kumar, M. Characterization and photoluminescence properties of some MLn₂(1-x)O₄: 2xEu³⁺ or 2xTb³⁺ systems (M = Ba or Sr, Ln = Gd or La). *J. Lumin.* **2011**, *131*, 587–591. [[CrossRef](#)]
33. Basavaraj, R.B.; Kumar, S.; Aarti, D.; Nagaraju, G.; Kumar, H.S.; Soundar, R.; Shashidhara, T.; Sumedha, H.; Shahsank, M. Color tunable orange-red light emitting Sm³⁺ doped BaZrO₃ nanopowders: Photoluminescence properties for w-LED applications. *Inorg. Chem. Commun.* **2021**, *128*, 108577. [[CrossRef](#)]
34. Navami, D.; Basavaraj, R.; Darshan, G.; Inamdar, H.K.; Sharma, S.; Premkumar, H.; Nagabhushana, H. Evolution of shapes and identification of level II and III features of fingerprints using CaZrO₃:Sm³⁺ fluorescent markers prepared via solution combustion route. *Opt. Mater.* **2019**, *88*, 479–487. [[CrossRef](#)]
35. Dewangan, P.; Bisen, D.; Brahme, N.; Sharma, S. Structural characterization and luminescence properties of Dy³⁺ doped Ca₃MgSi₂O₈ phosphors. *J. Alloys Compd.* **2019**, *777*, 423–433. [[CrossRef](#)]
36. Kumar, K.N.; Vijayalakshmi, L.; Hwang, P.; Wadhvani, A.D.; Choi, J. Bright red-luminescence of Eu³⁺ ion-activated La₁₀W₂₂O₈₁ microphosphors for noncytotoxic latent fingerprint imaging. *J. Alloys Compd.* **2020**, *840*, 155589. [[CrossRef](#)]
37. Babu, K.V.; Renuka, C.; Basavaraj, R.; Darshan, G.; Nagabhushana, H. One pot synthesis of TiO₂:Eu³⁺ hierarchical structures as a highly specific luminescent sensing probe for the visualization of latent fingerprints. *J. Rare Earths* **2019**, *37*, 134–144. [[CrossRef](#)]
38. Sodhi, G.; Kaur, J. Powder method for detecting latent fingerprints: A review. *Forensic Sci. Int.* **2001**, *120*, 172–176. [[CrossRef](#)]
39. Li, Y.; Hu, X.; Yao, H.; Ye, Y.; Zhou, J. Development of latent fingerprints by degradable highly-adhering powder—A long-term strategy for the fading of fingerprint residues. *Dye. Pigment.* **2023**, *219*, 111597. [[CrossRef](#)]
40. Di, L.; Xing, Y.; Yang, Z.; Li, C.; Yu, Z.; Wang, X.; Xia, Z. High-definition and robust visualization of latent fingerprints utilizing ultrabright aggregation-induced emission of iridium developer. *Talanta* **2023**, *264*, 124775. [[CrossRef](#)]

Disclaimer/Publisher's Note: The statements, opinions and data contained in all publications are solely those of the individual author(s) and contributor(s) and not of MDPI and/or the editor(s). MDPI and/or the editor(s) disclaim responsibility for any injury to people or property resulting from any ideas, methods, instructions or products referred to in the content.